AIAA/AAS Astrodynamics Specialist Conference
2 - 5 August 2010, Toronto, Ontario Canada

AIAA 2010-7969

Parachute triggering algorithms for re-entry vehicles

Barend E. Ording[1]
Delft University of Technology, Delft, The Netherlands

Martins Sudars[2]
Thales Alenia Space, Turin, Italy

and

Geert F. Brouwer[3]
Delft University of Technology, Delft, The Netherlands

Most re-entry vehicles utilize a Descent and Landing System (DLS) for a safe descent through the lowest part of the atmosphere. It usually requires deployment in a certain suitable range of flight conditions, which has to be estimated by limited means of navigation. This paper presents a comparison of currently used trigger methods and triggering algorithms which are based on correlation between in-flight measurements and the DLS triggering conditions, where the correlations have been extracted by multiple Monte Carlo campaigns. This approach gives a significant improvement of triggering accuracy over direct measurements for a ballistic re-entry. Also a lateral g-load safety trigger is developed to prevent the angle of attack oscillation escalation. Furthermore a sensor sensitivity analysis is performed for a lifting entry trajectory in order to support an upcoming ESA re-entry mission. The velocity drift appears to be the dominant dispersion by a factor ten for Mach estimation. Finally a case study has been performed to investigate the possibility to reduce the footprint by a dynamic parachute opening window. This could be effective for Mars re-entry using a parachute able to deploy beyond Mach 2.5, which would reduce the footprint by up to several tens of kilometers.

Nomenclature

AoA	=	Angle of attack
C_A	=	Longitudinal axis aerodynamic force coefficient
DLS	=	Descent and Landing System
IMU	=	Inertial Measurement Unit
M	=	Mach number
m	=	Vehicle mass
MC	=	Monte Carlo
PDF	=	Probability Density Function
R	=	Coefficient of determination
S_{ref}	=	Vehicle reference surface
V	=	Vehicle velocity
Γ	=	Longitudinal non-gravitational acceleration
ρ	=	Air density
σ	=	Standard deviation

[1] MSc student, Space Systems Engineering, Kluyverweg 1, 2629 HS Delft, The Netherlands, AIAA student member.
[2] Flight Dynamics Engineer, dep. Space Infrastructure and Transportation, Strada Antica di Collegno 253, Turin, Italy, AIAA member.
[3] Scientific staff, Space Systems Engineering, Kluyverweg 1, 2629 HS Delft, The Netherlands.

I. Introduction

Most re-entry vehicles utilize a Descent and Landing System (DLS) for a safe descent through the lowest part of the atmosphere. It usually requires deployment in a certain suitable range of flight conditions. The investigation goal is to find a simple, suitable, and precise solution to DLS system activation, whereas the deployment window may be very limited and the re-entry vehicles may not employ advanced navigation systems. This DLS trigger system can range from a simple preset timer to much more complex system, employing multiple sensors and capability to respond to off-nominal flight conditions. Determination of the deployment conditions and constraints may not be straightforward and must be estimated onboard the vehicle by combining various measurements. However adding complexity might lead to a more versatile system, but might reduce reliability.

II. Scope

This paper reflects a theoretical investigation carried out at Thales Alenia Space Italy in cooperation with Delft University of Technology in order to improve the DLS triggering algorithms for ballistic flight and to set a baseline for a lifting re-entry flight in order to support the existing and upcoming European re-entry vehicle missions. Due to their mission characteristics the ballistic and lifting re-entry vehicles have been considered separately.

The DLS triggering architecture must be designed in a way to guarantee the DLS operation in its qualification range and minimum possible flight parameter dispersions in order to increase the mission success. The performance and reliability is assessed by Monte Carlo simulation campaigns where a set of 3 or 6 degree-of-freedom trajectory simulations have been performed by an in-house high-fidelity flight mechanics simulation tool on real mission derived re-entry vehicles. Part of the work is devoted to studies of possible landing footprint size reduction by utilization of advanced navigation systems and high-mach supersonic drogues. This should be beneficial for recovery operations on earth and landing accuracy on other planets

III. Modeling

The re-entry trajectory and the sensors are to be modeled. The modeling of the re-entry is performed by FMST, 'Flight Mechanics Simulation Tool'[11]. FMST is a Matlab coded package, which has preset vehicle models, gravity and atmospheric models in order to perform trajectory simulations, batch and Monte Carlo analysis of aerospace vehicles. Sensor models are coded into the FMST package. To estimate the system performance, the uncertainties and their sources must be introduced in order to create realistic inputs for the study cases. There are three kinds of uncertainties in this model:

1. Measurement errors of sensors due to bias, bias drift and noise.
2. Modeling errors. Vehicle's inertial and aerodynamic properties, trajectory and environment are based on assumptions, wind tunnel data and models.
3. Initial condition dispersion due to injection uncertainties such as velocity, position as well as residual attitude and rates.

For a wide investigation of algorithms, it is assumed the vehicle can be equipped with different types of sensors; 3-axis accelerometers, g-switches, gyros, air data probes and pressure gauges. Using the properties of these measurements during the trajectory, the accuracy of these measurements is determined. GPS is not used as primary sensor due to its insufficient reliability due to the blackout and the fact it cannot be used on other planets. The lifting body should be able to estimate or measure its attitude, velocity and position vectors based on its inertial or hybrid navigation system. The parachute can be triggered by sensors thresholds, peak values, integral values, or combinations in cooperation with other sensors and timers. Specifically, the 6 degree of freedom simulations have revealed that vehicle's angle of attack oscillations and trim angle deviations can have major impact on the DLS system triggering conditions and performance.

IV. Ballistic re-entry algorithms

For the ballistic re-entry 22 triggering logics have been analyzed with measurement of g-loads, dynamic and static pressure. A specific feature of the developed algorithms is their correlation to the dispersions, in order to adapt to the specific flown trajectory within the band of uncertainty. These correlations are obtained by two measurements along the trajectory and then correlated to the time required to reach the desired deployment conditions.

A. Correlated algorithm development

Figure 1 on the left, shows a g-load curve of a ballistic re-entry with the investigated points of interest. On the right side a correlation example is given; the g-load threshold time difference between point 7 and 8 (t1) is correlated with the time to deployment indicated for the nominal trajectory at point 9 and the threshold at point 8 (t2). After selection of a specific correlation principle, Monte Carlo analysis can be used again to optimize the threshold values, e.g. 8 g to 6 g, 8 g to 5 g, 7 g to 5 g etc.

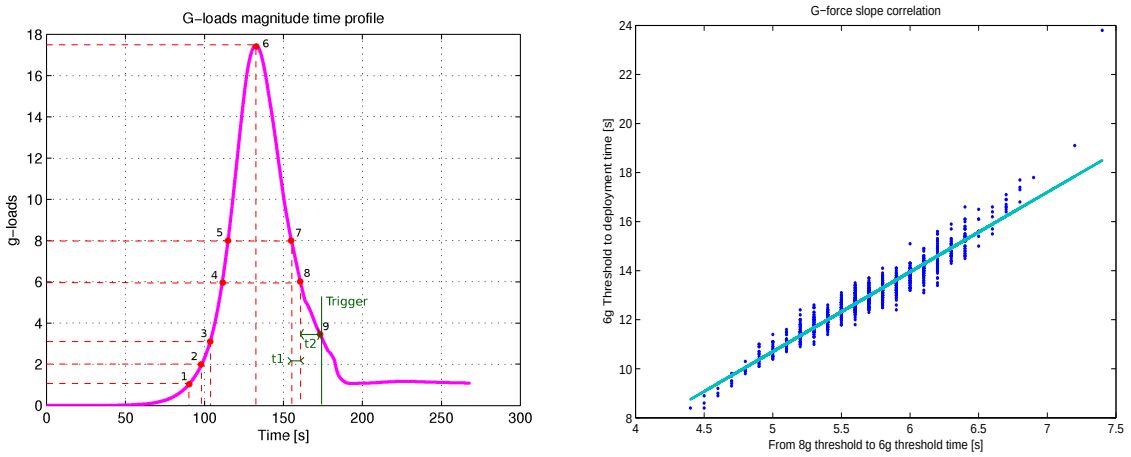

Figure 1. G-load correlation points of interest. *On the left side the re-entry g-load curve is depicted with 8 points of interest and the deployment point 9. On the right, a correlation of the time from point 7 to 8 is shown from the Monte Carlo analysis.*

This correlation is coded to an algorithm from which the flow diagram is displayed in Figure 2. These simple linear logics can be obtained by a microcontroller or by an analogue board, form which capacitors and resistors are sufficient to build a timer and linear regression. Such simplicity is desired in order to provide a high reliability of the system. All these algorithms contain a time interval measurement and a correlation, which calculates the time from the measured time interval to the deployment time, which depends on the dispersions. After the interval measurement is completed, at least 10 seconds are available for calculation and possible signal noise suppression. A further advantage of introduction of a time delay before the deployment is the elimination of measurement errors induced by the angle of attack oscillations, which remain small above Mach 2, for this reason it is beneficial to measure not at the last second, but at the point where the vehicle is the most stable, and the correlation is the highest.

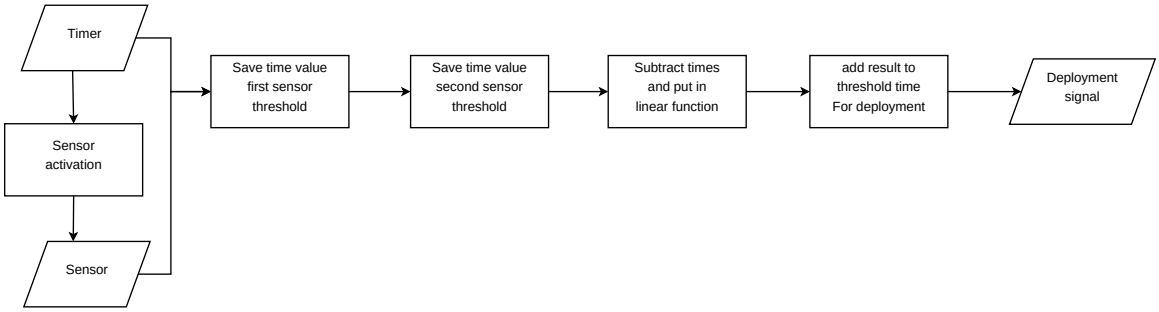

Figure 2. Algorithm flow diagram. *This figure shows which steps a correlated triggering algorithm is programmed to do, as soon as it is activated.*

B. Algorithm accuracy results

When different measurement methods are compared, g-load measurements and dynamic pressure measurements are similar performing and outperforming barometric measurements by almost a factor of 2 on accuracy. However, since it will be very difficult to directly measure the dynamic pressure, the latter one is discarded. Drag derived measurements might be suitable to estimate dynamic pressure, however, this is a pseudo measurement derived from the g-loads, for which direct correlation to the g-loads are then preferred. These correlated algorithms are compared to single threshold triggers in order to measure their performance, while still excluding sensor noise. Figure 3 shows

the Mach number dispersion such a single threshold case and to the best performing correlated algorithm, which is the correlation of two g-load thresholds at the end of the trajectory, which is basically a measurement of the g-load slope.

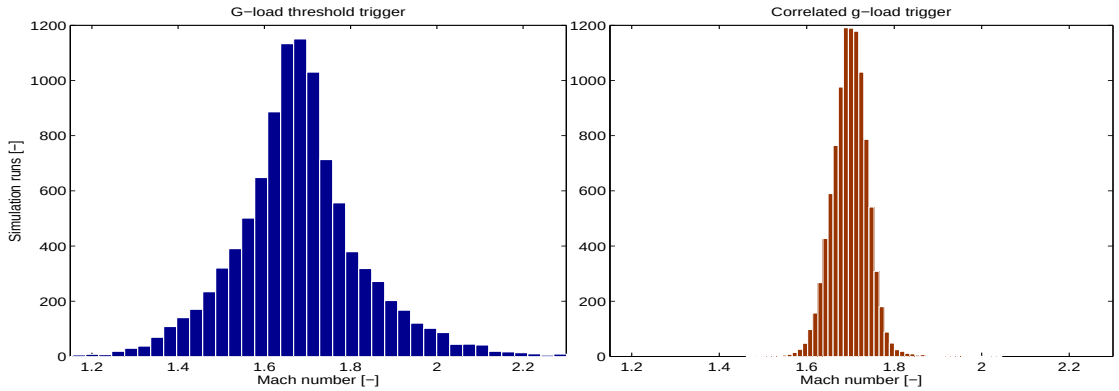

Figure 3. Parachute trigger Mach dispersions. *On the left side the Mach dispersion of a single threshold trigger is shown, the right side shows the dispersion of a correlated algorithm.*

The Figure shows a clear increase in accuracy of the correlated algorithm. If the distribution is approached to be Gaussian, a simple timer has a Mach dispersion of 0.79 3σ, the single threshold trigger a dispersion of 0.44 3σ and the correlated algorithm had a dispersion of 0.12 3σ. Static pressure measurements show similar improvement, a Mach dispersion of 0.55 3σ is obtained by a single barometric measurement, whereas a Mach dispersion of 0.22 3σ is obtained by a correlated barometric algorithm. Figure 4 shows similar results on the altitude dispersion. The increase of accuracy is less than the Mach estimation, because the correlated algorithm is correlated to the Mach values. The Mach number was chosen to be optimized, because in the study case mission, the Mach opening window was the smallest and therefore the most critical. The altitude dispersions for a timer, a threshold and the g-slope correlation are 2198, 1707 and 996 m 3σ respectively.

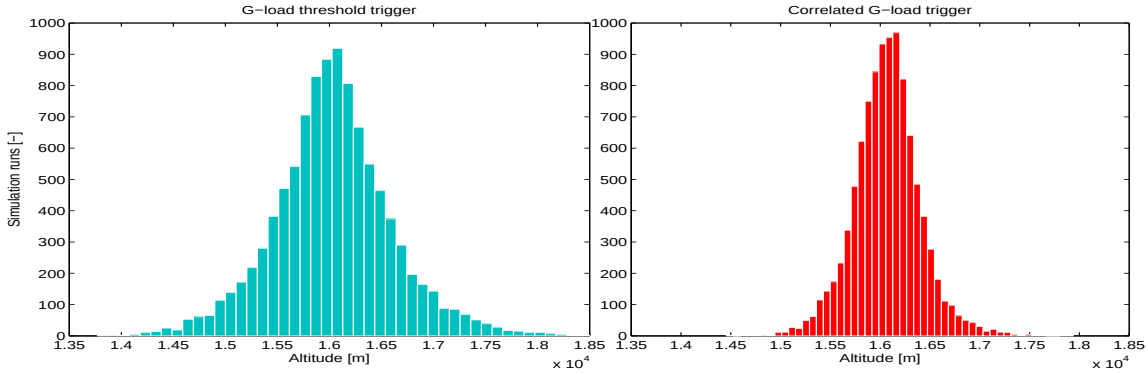

Figure 4. Parachute trigger altitude dispersions. *On the left side the altitude dispersion of a single threshold trigger is shown, the right side shows the dispersion of a correlated algorithm.*

C. High fidelity modeling

After a first selection round, the best performing architectures high fidelity models are developed and tested. High fidelity models are Simulink based models where the behavior of various sensors and data processing units has been simulated, including measurement noise and bias. Figure 5 shows the output of the high fidelity model trigger. Since there is a time delay build in, post processing can be performed to filter the noise. A 10 point moving average proved to be sufficient to eliminate most of the noise.

For off-nominal performance testing, a de-orbit malfunction is simulated by increasing the flight path angle dispersion up to 1 deg 3σ and a velocity dispersion of 130 m/s uniform. A single Monte Carlo run is performed with 0.1 g sensor noise and the result is displayed in Figure 5: Because the algorithm is adaptive and well correlated to flight path angle dispersions, the algorithm is able to stay within the parachute opening window, whereas uncorrelated algorithms would have a high probability of triggering outside the deployment window and inducing parachute failure.

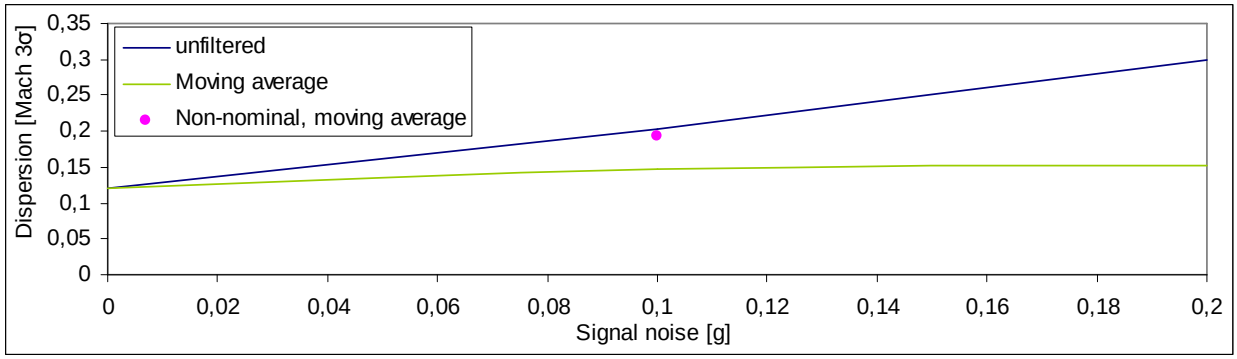

Figure 5. Mach dispersion as a function of the sensor noise. *A moving average noise filter can be applied because there is a time delay which allows post-processing which can effectively reduce the noise*

D. Lateral g-load triggering

Besides the well familiar g-load and the correlation based triggering techniques, additional criteria may be employed to guarantee the mission success. Many of the ballistic re-entry capsules are known to become unstable in transonic speeds. Knowing that aerodynamic uncertainties exist, the DLS triggering window may overlap the range where instability phenomena may occur leading to high angle of attack oscillations. These oscillations induce lateral g-loads which can be used to activate a safety trigger. Usually for capsules a small variation of angle of attack causes positive or negative normal force variations, which at certain angle of attack exceed those ones encountered prior to instability. If a lateral load algorithm is combined with another baseline algorithm (such as timer or axial g-load based which prevents from early triggering), a safe triggering range can be easily achieved by utilization of simple mathematical operations (such as absolute value) and logics, which can be also realized without utilization of digital signal processing devices.

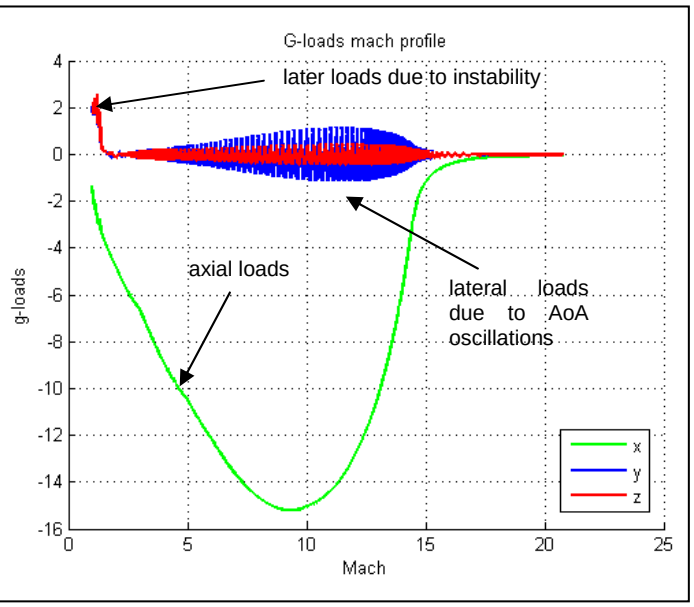

Figure 6. G-loads vs Mach number profiles projected on vehicle's body axis.

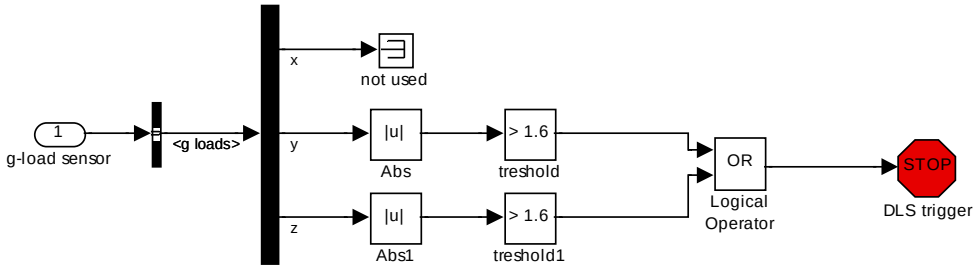

Figure 7 Later g-load trigger – very simple architecture.

The following examples illustrate results from MC simulations of vehicle, which is similar to European EXPERT re-entry capsule. A timer has been selected as baseline triggering criteria. Figure 8 and Figure 9 illustrate the results if DLS got activated only based on the lateral g-load triggering criteria. Figure 9 and Figure 10 illustrate results in combination with the baseline triggering criteria – timer. The results are based on 1000 Monte Carlo simulations, taking into account all missions' uncertainties. The lateral g-load triggering criteria works particularly

good if the slope of axis coefficient with respect to angle of attack is linear up to maximum AoA which can be tolerated by the DLS (so, for conical re-entry vehicles).

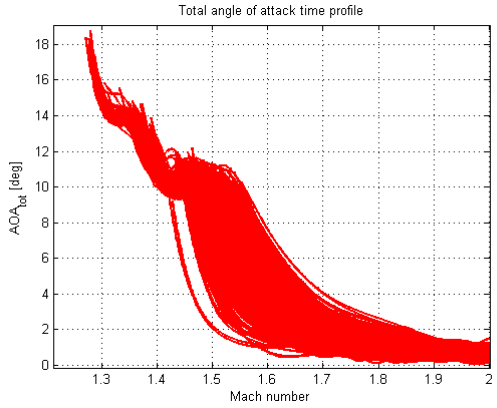

Figure 8. 1000 MC results of angle of attack versus mach number plots. *Angle of attack instability in certain circumstances may occur before DRS triggering*

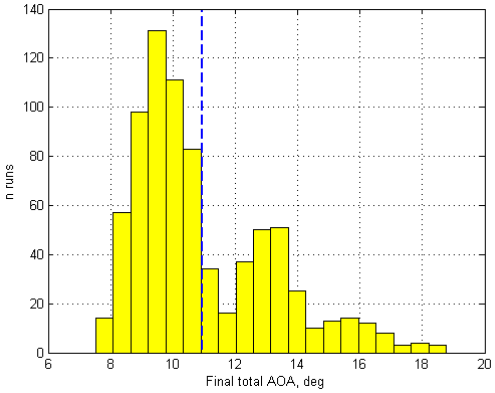

Figure 9. Histogram of AoA at triggering. *Lateral g-load trigger limits the angle of attack values. The shape of histogram depends on vehicle's aerodynamic behavior.*

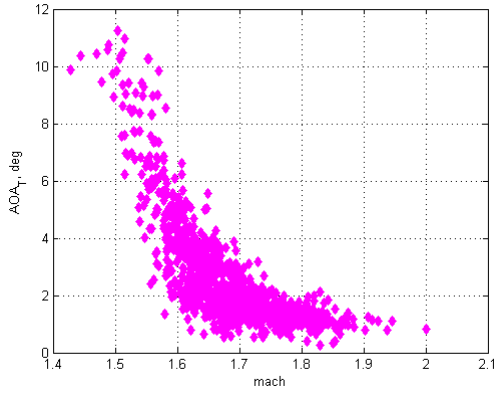

Figure 10. Angle of attack versus mach number at the moment of DLS triggering.

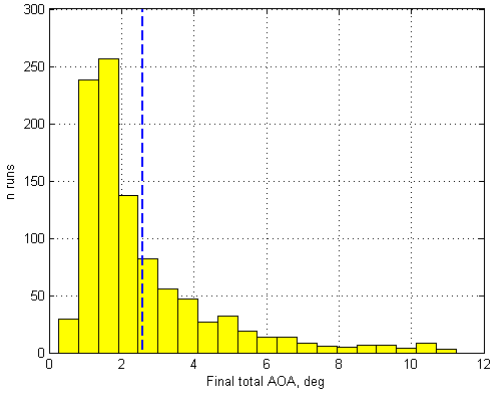

Figure 11. Histogram of angle of attack at triggering moment.

E. Conclusions for ballistic re-entry triggering

Using correlated algorithms improves the accuracy, but it is a function of the chosen types of dispersions. Performance of the algorithms will vary for every different case. These algorithms can be build with g-switches and simple electronics, but can also be used with an IMU and a processing unit. The time delay between the measurement and the deployment allows processing time for noise reduction. To prevent AoA oscillation escalation, measuring above Mach 2 is beneficial; alternatively lateral g-load triggering can be used.

V. Lifting re-entry trajectory

A lifting re-entry parachute trigger requires a different approach with respect to ballistic capsules, because the vehicle is actively controlled during the re-entry phase. This means the measured conditions cannot be correlated to specific initial flight conditions. These maneuvers can bee seen in Figure 12 on the left, which shows the nominal g-loads profile of the entire flight until the parachute deployment. The peaks in this curve are due to maneuvering and are not pre-determined. Also static pressure triggering will be inaccurate, because the deployment at a specified Mach number is not correlated to a specific static pressure and the pressure rate is too small. This is displayed in Figure 12 on the right, showing 10 Monte Carlo simulations for the supersonic phase of the flight. For these reasons continuous data acquisition and processing is required.

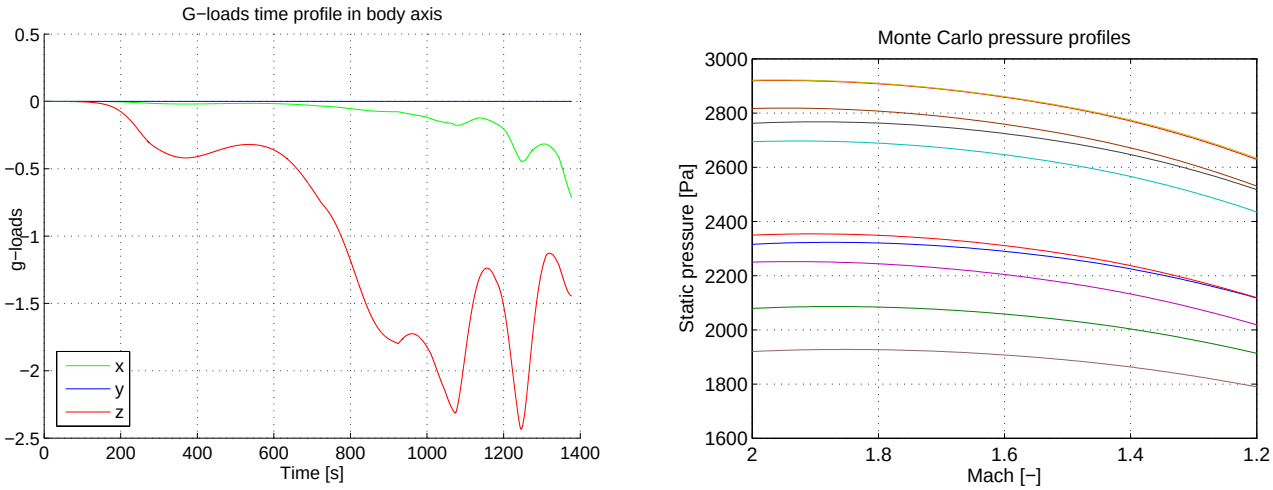

Figure 12. Lifting re-entry profiles. *On the left the g-loads are displayed, showing the g-load peaks due to roll and bank maneuvers. On the right, ten Monte Carlo profiles show that the supersonic regime can be at very different pressure environments.*

A. Drag derived Mach estimation

A method to estimate flight conditions with a non intrusive measurement is drag derived (altitude) (DD(A)). The DDA measurement is a means of estimating the altitude by combining the measurements of aerodynamic (or non-gravitational) accelerations, aerodynamic and atmospheric models[3]. With the altitude estimation the standard atmospheric temperature and thus the Mach number can be estimated. The non-gravitational component of the deceleration is extracted from the IMU (x-direction, Figure 12) and together with the vehicle's mass, reference area, its longitudinal axis aerodynamic force coefficient and the integrated velocity; the air density can be estimated using Eq.(1) . Using a standard atmosphere profile, an estimation of the altitude can be made.

$$P_{dyn} \approx \frac{m \cdot \Gamma}{S_{ref} \cdot C_A} = \tfrac{1}{2} \cdot \rho \cdot V^2 \tag{1}$$

Using the standard atmosphere profile, also the standard atmosphere temperature can be used in order to estimate the vehicle's Mach number. Using this drag derived measurement method, the altitude, dynamic pressure and Mach number can be determined, which are the parameters which define the parachute opening window.

A sensitivity analysis is performed to determine the dominant error in the drag derived Mach estimation. The following sensor errors are investigated:

- G-force measurement noise
- Velocity estimate drift
- Angle of attack estimate bias
- Velocity measurement noise

It appears the velocity drift is a dominant error by factor 10 compared to other sensor errors. For selection of the IMU, this velocity drift will be the driving parameter. Unfortunately, also a wind vector superimposed with the velocity measured drift. The Mach estimation dispersion induced by the velocity drift is presented in Figure 13. The error due to the aerodynamic uncertainty of the axial drag coefficient is small since a large estimation error of 20% of the density will induce an altitude error of less than 1.5 km because the density is exponential. This induces only a 1 K error on the atmospheric temperature if deployment is in or above the tropopause.

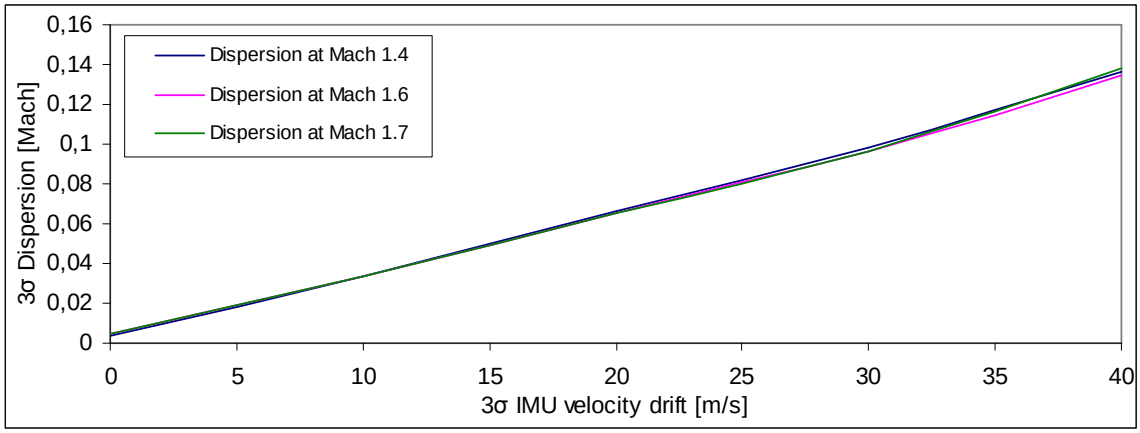

Figure 13. Mach dispersion as a function of the IMU velocity drift. *The IMU velocity drift is almost completely responsible for the Mach estimation error.*

B. Constant temperature Mach estimation

If the drogue deployment is between 11 and 30 km altitude, a more simple Mach estimation method can be used. Since the temperature is very stable in the stratosphere and has a squire root relation with the speed of sound, the speed of sound can be assumed constant. In this case, drag derived measurements are not required and only the velocity has to be known, which can be divided by a constant speed of sound to estimate the Mach number. Furthermore, the parachute deployment has to be performed at only one instant on which the temperature can be optimized to achieve similar performance as the drag derived measurements. Using Monte Carlo simulations this leads to a 3σ result of Mach 0.0678 for a velocity bias of 20 m/s, which is the same for a drag derived measurement. Figure 14 shows for both Mach estimation methods their estimation on the nominal trajectory.

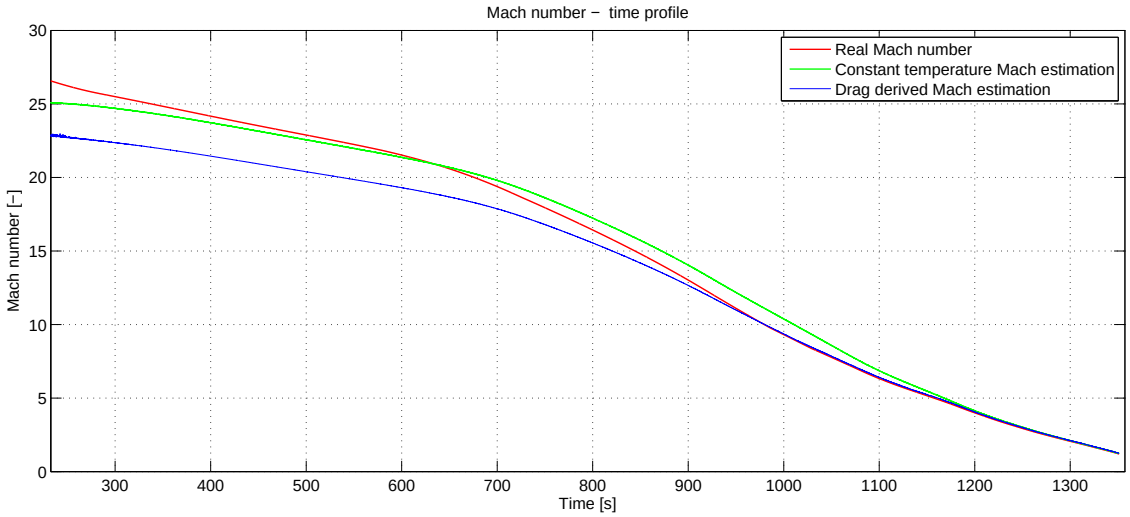

Figure 14. Lifting re-entry Mach profile with Mach estimation methods. *Both Mach estimation profiles will converge to an acceptable error below Mach 5, which is more than sufficient for parachute deployment.*

VI. Footprint Reduction investigation

If the flight conditions can be estimated accurately, the parachute opening window size might be used to open the parachute prior or post the nominal conditions in order to reduce the footprint of the re-entry vehicle's landing site. This way the longitudinal axis of the ellipse can be decreased. Furthermore it will be investigated whether a more robust parachute can make a significant reduction of the landing site footprint in order to have a semi-controlled re-entry. Such a controlled deployment might be an intermediate step from the uncontrolled ballistic flight and lift-vector control used for a completely guided re-entry.

A. Applicability for footprint reduction study

The investigation for footprint reduction by a dynamic parachute opening window aims on to investigate the opportunities and limitations of such a method. It could be used for precision landings for small footprints or as a simple reduction of large footprints. A precision landing would be possible if the footprint size is a similar size as the reduction possible by the dynamic parachute deployment. Unfortunately this is not the case, the footprint size of the re-entry missions investigated are at least more than twice the possible reduction size by a parachute in ideal circumstances. For this reason, a simple reduction method is investigated to reduce footprints in the order of tens of kilometers, while this will also give an insight what would be a feasible footprint size for precision landings.

B. Footprint reduction deployment control

From early analysis it was determined that even with a very robust drogue, the footprint can never be reduced to a theoretical zero, because the amount of kilometers reduction achievable by an adaptable drogue deployment time will never be at the same size of current re-entry footprints. For this reason, the deployment algorithm does not have to make a very fine estimation of the right moment of deployment: Defining three discrete instants of deployment is already sufficient to have a theoretical reduction of 66.7 % compared to a single point deployment on nominal conditions. So, the algorithm will be developed to define just 3 'settings': 1) 'flight path undershoot', 2) 'on nominal course', and 3) 'flight path overshoot'. The control algorithm will deploy at a defined high Mach number when the vehicle's flight path to overshoot its landing site and will deploy at a lower bound mach number when the vehicle is defined to undershoot its nominal landing site. This will keep the algorithm simple and more importantly, makes it possible to make a very course, and thus an easy to estimate, downrange prediction. For the footprint analysis again the Mach range is determined to be the driving parameter.

C. Footprint reduction on earth re-entry

An investigation has been performed on a 'generic' earth ballistic re-entry mission. The end part of the trajectory is plotted in Figure 15. The difference in distance covered between Mach 3 and 1.5 is around 4 km; which would be about the maximum footprint reduction possible with a very robust drogue parachute. For a drogue having similar mach range capability as the upcoming ESA EXPERT mission, the total reduction possible would be around 1.5 km. With a footprint of more than 20 km, such a reduction does not prove itself of added value, without the development of hypersonic decelerators.

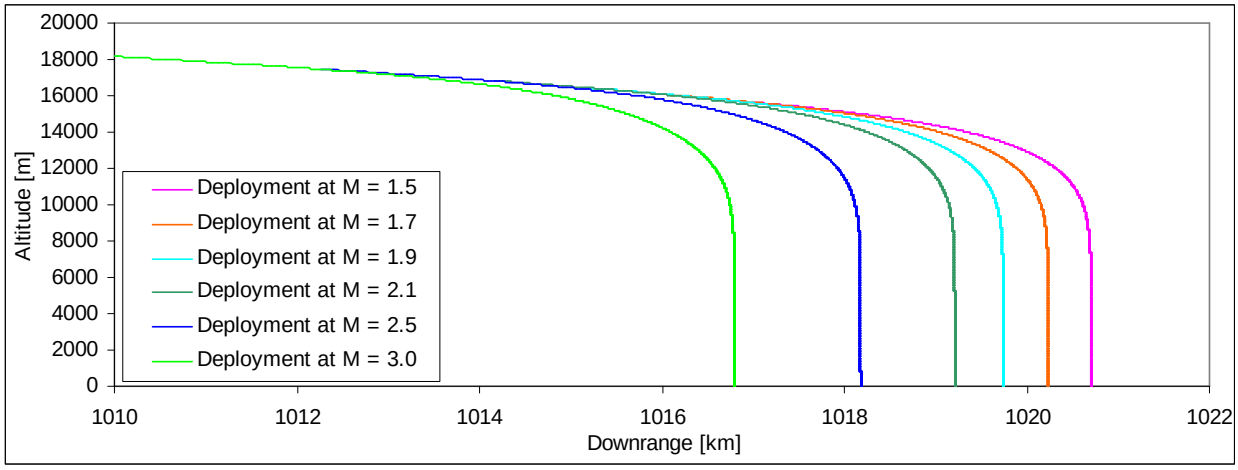

Figure 15. Terminal descent trajectory profiles with deployment at different Mach numbers.

D. MER footprint reduction case study

Mars has a rare atmosphere and low gravity compared to earth, these phenomena increase the distance flown in the supersonic regime. Footprints on Mars in general are bigger than on Earth because less is known about Martian atmosphere which has got a high variability, thus the modeling uncertainties atmosphere are also higher. Reduction of these footprints is desired in order to increase the probability of a landing on a flat area, which increases the probability of a mission success.

In order to make a realistic footprint reduction analysis, first a realistic re-entry scenario has to be set: Due to the availability of public data, the MER missions are selected to serve as a test scenario.For a first reconstruction attempt the results are very satisfying: Opportunity has landed within the determined landing ellipse and is 5.53 km

of the nominal determined landing point, see Figure 18. Unfortunately, Spirit has landed outside of the landing ellipse and is 19.20 km from the nominal landing point[13]. Also the determined deployment conditions can be reconstructed within a 5% error, except Spirit deployment altitude (14%)[13]. For a footprint reduction case study this reconstruction is sufficient, because the footprint performance is compared to the self made nominal case and not to the NASA determined footprint and real landing location.

To produce a baseline for a footprint reducing algorithm, the analysis is performed two times. The first analysis is based on deployment on exact knowledge of the vehicle's longitude. The sensor part is left out in this case in order to analyze the size of the footprint reduction possible by changing the deployment time, which is limited by the parachute's deployment capabilities in terms of Mach number. Acquiring position information during flight by sensors could be obtained by correlating ground images made during flight with a ground map database. This would be a new technology to be developed and for this reason a second analysis is performed. This analysis uses g-load correlations in order to predict the downrange flown and correct it by parachute deployment. This estimation is independent of navigational inputs. This results in an easy implementable algorithm, but has less footprint reduction performance.

The goal of the combination of this double analysis is to have an indication of the maximum footprint reduction achievable, which is limited to the parachute capabilities and to determine minimum footprint reduction requirements, which are driven by the navigation system capability. For the footprint reduction the trajectory of the MER-B vehicle (Opportunity) is used.

E. MER footprint reduction limited on parachute capabilities

The footprint reduction achievable is mainly a function of two related parameters; the Mach deployment window and the maximum deployment Mach number. The footprint reduction capability increases exponentially if the parachute's maximum Mach number is increased, because the Mach opening window will get larger, the velocity is higher so more distance can be covered and the flight path angle is shallower. This can be seen in the isobar plot of Figure 16. A higher Mach number deployment is also desirable to land at higher elevations on Mars[4]. Development of a parachute with a higher opening velocity than current Viking technology might be designed with both benefits in mind.

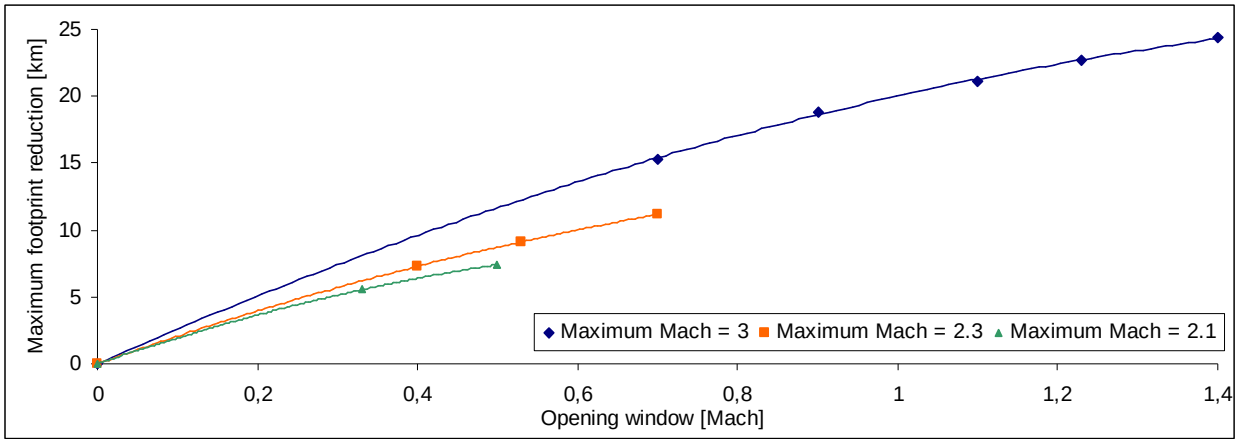

Figure 16. Maximum footprint reduction as function of the parachute opening Mach range and Maximum deployment Mach number. *The footprint reduction capability increases with a larger opening window and a higher maximum Mach number.*

F. MER footprint reduction using only g-load measurements

To specify minimum requirements, g-load correlations are used in order to define the desired instant of parachute deployment. As mentioned in paragraph VI B, only three settings are investigated to simplify the algorithm. So four correlations are needed:

1. A correlation to determine the downrange from the initial point, this is a function of the actual vehicle mass, aerodynamic uncertainties, the flight true flight path angle and most of all, the actual atmospheric conditions. For such an algorithm, no navigational errors can be corrected.
2. High velocity deployment, to compensate for overshoot
3. Nominal velocity deployment
4. Low velocity deployment, to compensated for undershoot

The g-load threshold correlations are shown in Figure 17. It can be seen that although no navigation input is added, the downrange can be predicted by correlating it with the time between g-load thresholds at an early phase during the re-entry with a R^2 of 0.81. The downrange is divided into an undershoot range, a nominal range and an overshoot range. These downrange prediction ranges activates one of the other 3 correlations which are used to determine the selected deployment Mach number similar as described in paragraph IV.

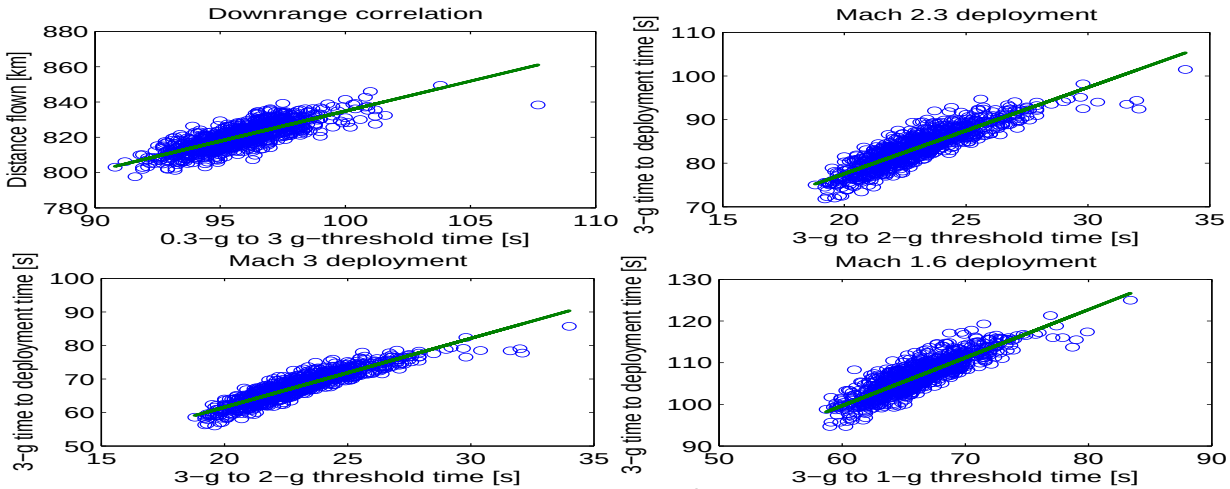

Figure 17. G-load correlations used for dynamic triggering. *R^2 vales are: 0.80 ,0.89 0.92,0.87 from upper left to right and down left to right respectivly.*

The correlated algorithms are capable of reducing the footprint from 53.51 km to 38.23 km, a reduction of 15.29 km, which is about 28.6 %. The footprint reduction can go up to 25 km, which is 48 % when additional navigation inputs are added. The results of a 10000 run Monte Carlo analysis are presented in Figure 18.

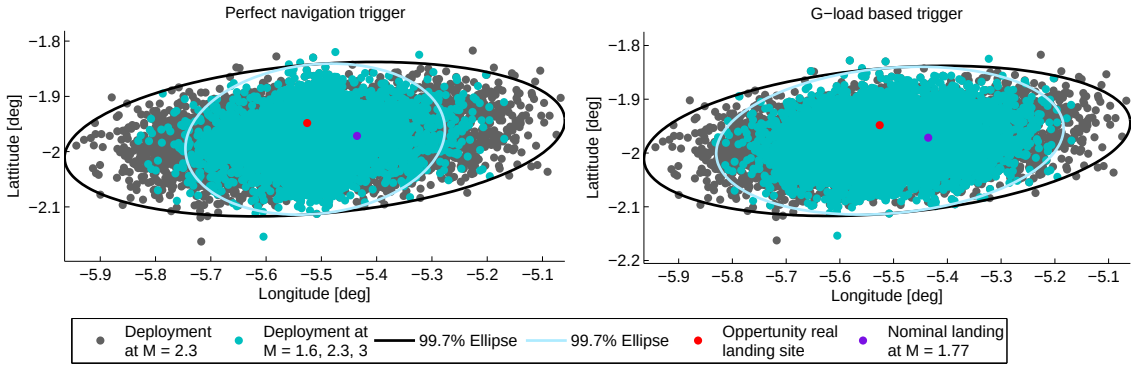

Figure 18. Footprint ellipses generated by Monte Carlo analysis. *The figure on the left shows the footprint reduction possible limited on the parachute capabilities, the right side figure shows the reduction possible using g-load correlations only.*

A remark must be made of the mathematical background of the generation of the 3σ ellipse. The developed ellipse is such that the 2-dimensional probability is 99.73%, assuming a Gaussian circular distribution[12]. However, the perfect navigation control algorithm creates stepwise changes in the simulation, which makes the PDF leptokurtic with a kurtosis of 6.15, whereas the nominal landing footprint has a slightly platykurtic PDF of 2.94.

VII. Conclusions

This parachute triggering investigation involved three cases, a ballistic re-entry and a lifting re-entry on Earth and a ballistic re-entry on Mars. For the earth ballistic re-entry it can be concluded that correlated algorithms outperform the current used threshold triggers on accuracy and the ability to adapt to off-nominal de-orbiting. Furthermore,

adding a time delay between the measurement and the actual deployment has the benefits of providing processing time for noise reduction and removing the axial g-load measurement error for possible angle of attack oscillations divergence. Alternatively, a lateral g-load trigger can be used to prevent angle of attack oscillation escalation.

For the lifting re-entry, drag derived measurements are found to be a very suitable non-intrusive measurement method to estimate deployment conditions. The velocity measurement by the IMU is the driving parameter for parachute triggering by a factor 10, compared to all other measured variables used for drag derived measurements. Furthermore, assuming a constant stratosphere temperature might already provide sufficiently accurate Mach estimation for parachute deployment. This removes extra calculation and measurement steps compared to the drag derived measurements.

Footprint reduction by the use of a dynamic opening window of the parachute is found to be ineffective on earth, but has potential on Mars. A reduction of 25 km could be achieved if current Viking parachute technology is stretched to a maximum Mach number of 3. A higher opening velocity is already desired in order to be able to land on the Martian highlands. Modified parachute designs can be developed to incorporate both benefits.

Acknowledgments

This research has been performed by the Delft University of Technology, together with Thales Alenia Space Italy in Turin. The first author gratefully acknowledges both entities for their flexibility in the cooperation, which made this cooperation a success. Furthermore the Erasmus Student Network is acknowledged for their financial support which allowed working on the industrial site.

References

[1]Crowley, G., M. A. Bullock, C. Freitas, D. Boice, L. Young, D. H. Grinspoon, R. Gladstone, R. Link and W. Huebner, *DEVELOPMENT OF A SURFACE-TO-EXOSPHERE MARS ATMOSPHERE MODEL.*, Southwest Research Institute, San Antonio, Texas, U.S.A.

[2]Gerald Pignie, Patrick Delaux, Laurent Bouaziz, Hamid Kebci, François Trinquard, *Parachute Opening Triggering Algorithm Of The Atmosperic Re-Entry Demonstrator*, Aiaa Gnc Conference, July 29-31 1996, San Diego, CA

[3]Giorgio Tumino, *The Ixv Project, The Esa Re-Entry System And Technolologies Demonstrator Paving The Way To European Autonomous Space Transportation And Exploration Endeavours*, IAC-08-D2.6.01

[4]Manning Robert M., Adler, Mark, *Landing on Mars*, AIAA Space 2005 Conference, California, Long Beach, AIAA-2005-6742

[5]Muylaert, Jean, Francesca Cipollini, Giorgio Tumino, Willi Kordulla, Giorgio Saccoccia, Constantinos Stavrinidis, *Preparing for Atmospheric Reentry with EXPERT's Help, An Aerothermodynamic In-Flight Research Programme*, esa bulletin 114, may 2003

[6]Myron R. Grover III, Benjamin D. Cichy, *Overview of the Phoenix Entry, Descent and Landing System Architecture*, Jet Propulsion Laboratory, California Institute of Technology, Pasadena, CA, 91109, USA

[7]NASA, *GENESIS*, Mishap Investigation Board Report, Volume I, NASA

[8]Paulat, J.C.; Boukhobza, P., *Re-entry Flight Experiments Lessons Learned – The Atmospheric Reentry Demonstrator ARD*, In Flight Experiments for Hypersonic Vehicle Development (pp. 10-1 – 10-46). Educational Notes RTO-EN-AVT-130, Paper 10. Neuilly-sur-Seine, France: RTO. Available from: http://www.rto.nato.int/abstracts.asp, 2007

[9]Philip C. Knocke, Geoffrey G. Wawrzyniak, Brian M. Kennedy, *Mars Exploration Rovers Landing Dispersion Analysis*, AIAA/AAS Astrodynamics Specialist Conference and Exhibit, Providence, Rhode Island, 16-19 August 2004, AIAA 2004-5093

[10]Prasun N. Desai, Robert A. Mitcheltree, F. McNeil Cheatwood, *Entry Dispersion Analysis For The Stardust Comet Sample Return Capsule*, NASA Langley Research Center

[11]Sudars M., A.Saluzzi, *Modeling of Parachute Dynamics in a Synthetic Flight Mechanics Simulations Environment*, AIAA-2009-2943

[12]Wayne E. Hoover, *Algorithms For Confidence Circles and Ellipses*, NOAA Technical Report NOS 107 C&GS 3, Charting and Geodetic Services, Rockville, MD, September 1984

[13]Withers, Paul a., Michael D. Smith b, *Atmospheric entry profiles from the Mars Exploration Rovers Spirit and Opportunity*, Center for Space Physics, Boston University, USA, Elsevier, Icarus 185 (2006) 133-142